


Article

Assessing Influential Factors on Inland Property Damage from Gulf of Mexico Tropical Cyclones in the United States

Shaikh Abdullah Al Rifat ¹ , Jason C. Senkbeil ² and Weibo Liu ^{1,*} 

¹ Department of Geosciences, Florida Atlantic University, Boca Raton, FL 33431, USA; srifat2017@fau.edu

² Department of Geography, University of Alabama, Tuscaloosa, AL 35487, USA; jcsenkbeil@ua.edu

* Correspondence: liuw@fau.edu; Tel.: +1-561-297-4965

Abstract: The Gulf and southeast coastal communities in the United States are particularly vulnerable to tropical cyclones. Coastal areas generally receive the greatest economic losses from tropical cyclones; however, research suggests that losses in the inland zone can occasionally be higher than the coastal zone. Previous research assessing the inland impacts from tropical cyclones was limited to the areas that are adjacent to the coastal zone only, where losses are usually higher. In this study, we assessed the spatial distribution of inland property damage caused by tropical cyclones. We included all the inland counties that fall within the inland zone in the states of Louisiana, Mississippi, and Alabama. Additionally, different factors, including meteorological storm characteristics (tropical cyclone wind and rain), elevation, and county social-economic vulnerability (county social vulnerability index and GDP) were assessed to measure their influence on property damage, using both ordinary least squares (OLS) and geographically weighted regression (GWR) models. GWR performs better than the OLS, signifying the importance of considering spatial variations in the explanation of inland property damage. Results from the tristate region suggest that wind was the strongest predictor of property damage in OLS and one of the major contributing factors of property damage in the GWR model. These results could be beneficial for emergency managers and policymakers when considering the inland impacts of tropical cyclones.

Keywords: inland property damage; tropical cyclones; ordinary least squares (OLS); geographically weighted regression (GWR)



Citation: Rifat, S.A.A.; Senkbeil, J.C.; Liu, W. Assessing Influential Factors on Inland Property Damage from Gulf of Mexico Tropical Cyclones in the United States. *ISPRS Int. J. Geo-Inf.* **2021**, *10*, 295.
<https://doi.org/10.3390/ijgi10050295>

Academic Editors: Dean Kyne and Wolfgang Kainz

Received: 23 March 2021

Accepted: 26 April 2021

Published: 4 May 2021

Publisher's Note: MDPI stays neutral with regard to jurisdictional claims in published maps and institutional affiliations.



Copyright: © 2021 by the authors. Licensee MDPI, Basel, Switzerland. This article is an open access article distributed under the terms and conditions of the Creative Commons Attribution (CC BY) license (<https://creativecommons.org/licenses/by/4.0/>).

1. Introduction

Tropical cyclones (TCs) are common phenomena around the world and affect almost all tropical regions [1]. On average, TC events caused an annual estimated global damage of USD 26 billion and 19,000 deaths over the last decade [2]. Future climate change may increase the intensity of TCs globally, and consequently could increase losses inflicted by TCs as evidenced in previous studies [3–5]. However, impacts from landfalling TCs are not limited to coastal areas only. TCs can maintain or even intensify farther inland and this is evidenced in different regions around the globe, including the United States (U.S.) [6–9].

During the period of 1970–2009, there were many deadly (1970 cyclone in Bangladesh) and costly (2005 Hurricane Katrina in the U.S.) TCs [1]. The cumulative death toll inflicted by TCs globally during this period was around 800,000. Over the last two decades, property damage caused by TCs is estimated at over USD 946 billion worldwide, which is almost one-third of all the damages caused by natural disasters during this period [10]. Losses from tropical cyclones in the U.S. have risen over the past few decades [11–15]. However, when adjusted for inflation, economic losses have not increased nor has the frequency or intensity of tropical cyclones landfalls increased in the U.S. [16]. Coastal population density has rapidly increased, and this combined with almost 85% of the total tropical cyclone (TC) damage in the U.S. being caused by major hurricanes creates vulnerability and the potential for greater economic loss in the future [12]. The 2005 and 2017 seasons were

the most active and destructive hurricane seasons for the Atlantic Basin in recent years. Hurricane Katrina in 2005, the costliest disaster in U.S. history, alone caused around 1833 deaths, both directly and indirectly, and USD 108 billion in property loss in 2005 [17,18]. Damages caused by the 2017 hurricane season in the Atlantic basin are estimated to be more than USD 125 billion [19]. With increasing coastal and inland population, TC property damage is projected to increase if future TC frequency and intensity follow climate model projections [20–22].

Previous research mainly studied the impacts of TCs in the coastal regions where the impacts are often the highest. However, the impacts from landfalling TCs in the U.S. are frequently experienced inland where there are sizeable populations [23]. Although TCs generally weaken quickly after making landfall, inland impacts from landfalling TCs can be extensive. In recent years, most of the fatalities caused by TCs in the U.S. occurred in the inland counties compared to the coastal counties [24]. Rappaport (2000) [25] found that these losses of lives are often caused by hazards associated with TCs, including heavy rainfall, high winds, and TC-induced tornadoes.

TC fatalities and property loss can be influenced by the physical characteristics of a TC and the levels of social vulnerability of the population in the region impacted. There are many factors that influence social vulnerability [26–32]. Some of these common factors are organized under broader categories of age, gender, race/ethnicity, and socioeconomic status. More specifically, social vulnerability can be assessed through a combination of (1) a lack of access to resources, (2) limited access to political power and representation, (3) social networks and connections, (4) beliefs and customs, (5) building stock and age, (6) weak and physically limited individuals, and (7) type and density of infrastructure and lifelines [28].

Moreover, population increase is another critical factor for TC related losses [33,34]. The U.S. population is expected to reach 400 million by the year 2040 [35]. Consequently, the urban and suburban regions in the country, both in coastal and inland areas, are also expected to see a substantial increase in population [36]. Population increase enhances the increase in the built environment and developed footprint of an area, which increases the risks of potential impacts from geophysical hazards [33,34,37,38]. Socioeconomic factors are also considered to have significant impacts on TC damages [11,39]. Gross domestic product (GDP) per capita is considered one of the major factors of economic vulnerability to disasters [27,40]. Higher GDP per capita suggests lower vulnerability to disasters and corresponds to lower disaster impacts [41,42]. Other socioeconomic factors used in previous research include asset value, built environment, etc. [35,43].

The impact of TC physical characteristics on property loss and fatalities is well documented in the coastal zone but often overlooked inland [14]. Severe wind, tornadoes, and flooding due to heavy rainfall are the worst hazards associated with TCs as they move inland, with flooding being most destructive in the literature [44]. In particular, fatalities from freshwater flooding occur mainly in inland counties [25,45]. Czajkowski, Simmons, and Sutter (2011) [45] found that one-inch and one-knot increases in rainfall and wind increase total inland fatalities by 28% and 4%, respectively.

High winds associated with TCs are another lethal and costly hazard even though wind decreases in inland counties. Schmidlin (2009) [46] discussed 407 deaths from wind-related tree failures in the U.S. from 1995 to 2007, and many of these fatalities were associated with TCs in inland counties. Sporadic wind gust speeds can remain well above hurricane force for hundreds of km inland from landfall [47]. Recently, category 5 Hurricane Michael in 2018 caused hurricane force wind gusts of over 200 km inland [48]. A faster-moving TC produces high wind gusts farther inland since it arrives inland at a greater intensity [14,49]. TC-induced tornadoes are another inland wind threat [50,51]. Tornadoes cause significant property damage and 5% of overall TC related deaths [25].

Additionally, it is estimated that TC frequency and intensity will continue to increase due to future climate change as found in previous studies [21,22,52–54]. Generally, areas that are frequently hit by TCs are subject to higher property damages and fatalities. Fur-

thermore, physical characteristics of the areas impacted by TCs, such as elevation, can also play an important role in reducing the impacts from TCs, especially in inland areas. As mentioned earlier, freshwater flooding from rainfall associated with TCs is a major threat in inland areas. Higher elevation corresponds to a lower risk of flooding as found in previous studies [55,56].

The U.S. Gulf and southeast coasts are particularly vulnerable to TCs [57,58]. Burroughs (2007) [59] showed that TC related property damages in the U.S. Gulf and east coast could be USD 5 billion per year. The 2005 and 2017 Atlantic hurricane seasons produced 28 and 17 named TCs, respectively [60,61]. Additionally, recovery costs from the major hurricanes in this region were very expensive and hard to predict [62]. While previous studies have found that TC-related losses in the inland areas could be substantial, research investigating the factors that influence damage caused by landfalling Gulf of Mexico TCs in the Southeastern U.S. is still very limited, let alone focusing on the inland areas of this region. Additionally, research incorporating different factors (e.g., hazards associated with TCs, social and economic vulnerability, and physical characteristics of the areas impacted) that influence inland property damage caused by landfalling Gulf of Mexico TCs in this region has been minimal.

Another important issue is how to measure the impacts of different factors on TC related property damage. Previous studies measured the impacts of different factors on TC-caused property damage either for a single storm or with descriptive statistics and the global regression method [45,63–65]. However, disaster damage, including losses inflicted by TCs, varies across the space [66]. Therefore, the impacts of different factors contributing to TC-related property damage could also vary spatially. In this regard, geostatistical and spatial analyses methods could come in handy as they consider spatial statistical relationships between different variables. For example, García-Ayllón et al. (2019) [67] used bivariate spatial correlation to identify the spatial impacts of different factors on earthquake damage in Lorca, Spain. In addition, recent studies showed that spatial regression methods, such as geographically weighted regression (GWR), are capable of better explaining and capturing the spatial relationships between disaster damage and contributing factors [66,68,69]. Therefore, this research employs a spatial statistical approach to quantify the impacts of different influential factors to TC-related property damage. Nevertheless, we also used a global regression model to analyze and compare the results in this study.

Investigating the spatial distribution of inland property damages caused by TCs and how the relationships between TC-related inland damages and contributing factors vary spatially could provide emergency managers and policymakers with a tangible product to assist in overall disaster management planning in this region. To minimize these gaps in this field, the first goal of this research was to explore and understand the intersection of meteorological storm characteristics, physical characteristics of the areas impacted, and social-economic vulnerability variables as predictors of county-level inland property damage. Once these interactions were determined, the second goal was to see any spatial relationships between those factors and property damages in the inland counties.

2. Materials and Methods

2.1. Study Area

This study focuses on the inland counties of the Southeastern U.S. Six Southeastern states bordering both the Gulf of Mexico and the Atlantic Ocean (Texas, Louisiana, Mississippi, Alabama, Georgia, and South Carolina) were preliminarily selected as the study area for this research because these states are routinely hit by TCs. Florida was not included because all Florida counties are coastal as defined by this research, and this is described in the next section. Texas, Georgia, and South Carolina have an insufficient sample size of counties with inland property damage, so they were excluded. For these reasons, Alabama, Mississippi, and Louisiana were selected as the study area for this research.

Inland counties were defined as those that are adjacent to coastal counties and are not coastal counties according to the NHC definition [45]. However, inland damages due to landfalling TCs are not limited to the counties that are adjacent to the coastal counties only and it could expand farther inland. Therefore, we took a new approach to clearly identify the inland zone in this study. Senkbeil, Brommer, and Comstock (2011) [14] identified different post-landfall hazard zones (Surge zone, Coastal zone, Inland zone, and Continental zone). They identified the inland zone as six to twelve hours after landfall, based on an average forward speed of 16 km per hour. Using these criteria, the average forward speed of a hurricane was multiplied by six since hurricanes typically move into the Inland Zone after six hours of landfall. A 96 km buffer was created using the Geographic Information System (GIS) from the U.S. coastline boundary bordering the three states, Alabama, Mississippi, and Louisiana, to define the inland area. All the counties in this tri-state region that are located on the north side of this buffer line were marked as inland counties, and these counties are the final study area for this research. If the 96 km buffer line bisected a county, it was not included as an inland county. There are 170 inland counties totally in this study (Figure 1). This region typically has a warm and humid summer with a short winter that is generally mild to cold. The elevation in the study area ranges from 13.83 m to 371.59 m, and the average elevation is 110.62 m.

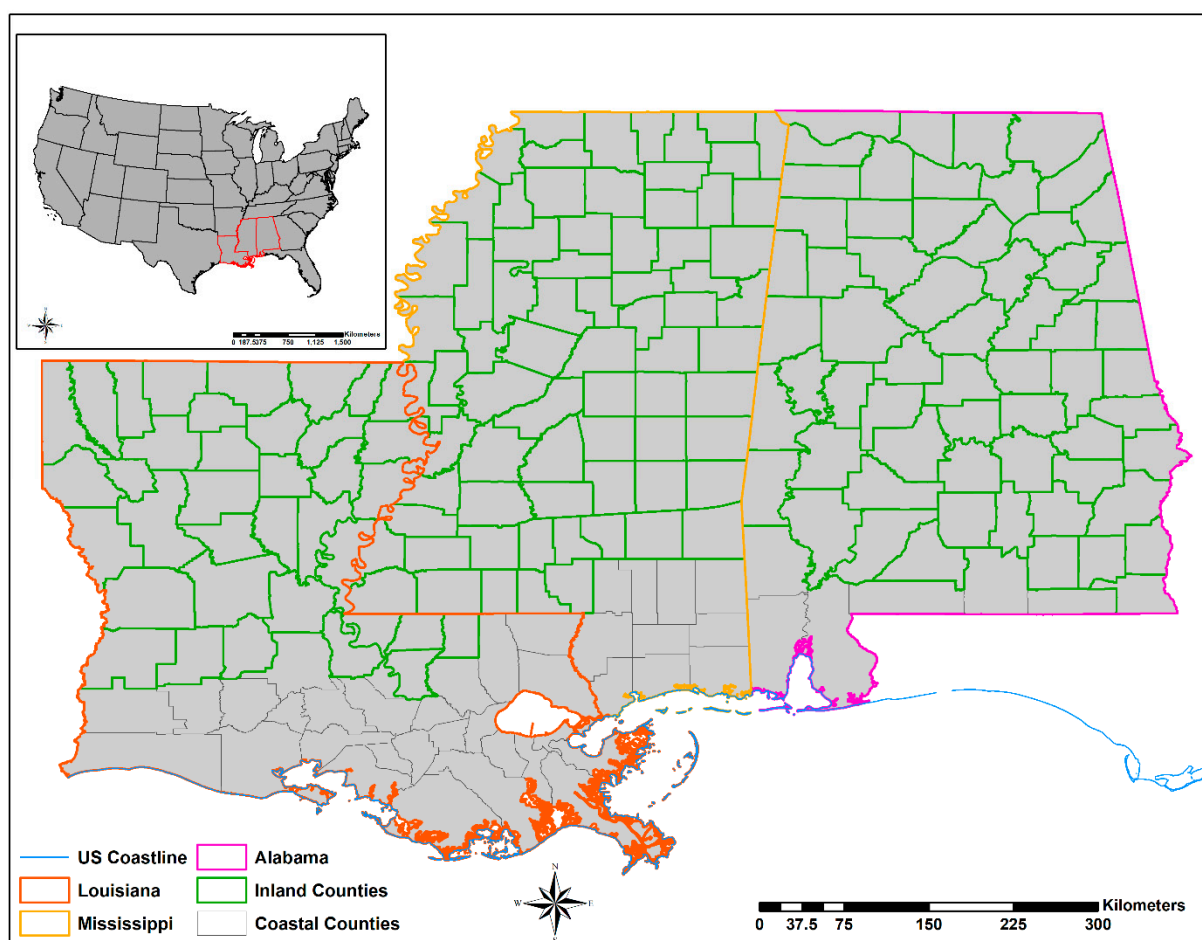


Figure 1. Inland counties in the study area along with the U.S. coastline.

2.2. Data

2.2.1. TC-Related Property Damage

County level property damage data for hurricanes and tropical storms were taken from the widely used Spatial Hazard Events and Losses Database for the U.S. (SHELDUS)

database (<https://cemhs.asu.edu/sheldus> accessed on 5 January 2021) [66,70]. SHELDUS contains an archive of monetary damage for each U.S. county for each type of natural hazard event beginning in 1960. Damage data include direct losses caused by an event (property and crop loss). The damage data obtained from SHELDUS were cross-checked against NOAA's (National Oceanic and Atmospheric Administration) Storm Data website. Several discrepancies were found for property damage caused by TCs between these two databases prior to 1996 at the county level. Therefore, the study period was selected between 1996 and 2018. Finally, since Hurricane Katrina was such an anomalous storm, it was excluded in this study following a similar approach [45].

2.2.2. Influential Factors

TC-related property damage is influenced by many factors. As mentioned earlier, TC-related loss is caused by different types of factors, including hazards associated with TCs, such as wind, rainfall, and tornadoes, physical characteristics of the area impacted, and socio-economic vulnerability. Based on previous studies, seven different factors were selected for this study that influence property damage, including TC wind, TC rainfall, TC frequency, county social vulnerability, mean elevation of the county, GDP per capita, and population density.

- TC tracks.

TCs that caused property damage in the study area during 1996–2018 were selected first. In doing this, historical hurricane tracks from NOAA's International Best Track Archive for Climate Stewardship (IBTrACS) website were downloaded. Then, only the storms that made landfall along the Gulf of Mexico and hit the study area in the study period were selected. These selected storms were matched with the SHELDUS database to make sure that all the damage-causing storms were selected in this study. There were 22 different tropical cyclones causing property damage in the study area between 1996 and 2018.

- TC rainfall.

Rainfall has been a primary variable associated with property damage from TCs. County rainfall data for each selected storm during the 22 years were collected from the Parameter-elevation Regressions on the Independent Slopes Model (PRISM) Climate Group website (<https://prism.oregonstate.edu/recent/> accessed on 5 January 2021). They used both Climatologically Aided Interpolation (CAI) and radar interpolation methods to interpolate the observed precipitation for the conterminous U.S. at 4 km spatial resolution. For this study, daily rainfall data were downloaded for each of the selected 22 storms, then the average values of the rainfall at the county-level were calculated for each storm in ArcGIS. When available, rainfall data from nearby weather stations were used to verify the accuracy of the PRISM precipitation data. Since hurricane rainfall rates are fairly constant 6 h after landfall in our tri-state study region [71], the PRISM estimates matched the observed rainfall well. Since observed rainfall was not available for most counties, the PRISM estimates were used for every county to be consistent. Finally, the average rainfall value for each storm were added together to calculate the total rainfall amount for the TCs at the county-level in our study area.

- TC wind.

Wind is also a primary physical variable that creates inland property damage. The county wind speed data were obtained by overlaying the IBTrACS historical TC tracks dataset onto the counties in our study area in ArcGIS. The IBTrACS historical TC tracks dataset stores maximum sustained wind (MSW) speed measurements in knots and three different wind speed radii, including 34, 50, and 64 knots for four quadrants, along with the latitude and longitude coordinates for the entire center of the storm path. We made several modifications to these data to calculate the county-level wind speed for the selected TCs. First, the MSW stored in conjunction with the latitude and longitude coordinates of the center of the storms were retained for the counties the center of each storm crossed.

Secondly, using the quadrant radii field for three different wind speed values (34, 50, and 64 knots), buffers were created for those three wind speeds separately and for each storm in ArcGIS. Finally, the highest value of the wind for each county for each TC was considered in this research. For example, if a county falls within the buffer zones of both 64 knots wind speed and 50 knots wind speed for a storm, that county was assigned the highest wind value of 64 knots for that particular storm. The wind values for all storms were added together to calculate the total wind value (in knots) for each inland county.

- County social vulnerability.

As we discussed earlier, social vulnerability has been associated with disaster losses [29]. The social vulnerability assessment highlights the counties where a high concentration of people who are socially vulnerable to environmental hazards is located within the study area. For this study, the Social Vulnerability Index (SoVI) for the year 2014 was used from the Hazards and Vulnerability Research Institute at University of South Carolina for quantifying county social vulnerability. To prepare the SoVI in the U.S., they first identified 29 variables reflecting social vulnerability, and used principal component analysis to identify eight significant components of social vulnerability. Each component was given a score for each county in the U.S. and then summed together to get a composite social vulnerability score. Each county was given a percentile score (1 means least vulnerable and 100 means most vulnerable) which represents that county's overall social vulnerability. In this research, this percentile score for county social vulnerability was used for each inland county.

- Elevation.

In this study, the average elevation of the counties was selected as one of the major factors that influence the property damage caused by TCs. Previous studies have shown that higher elevation areas have lower damages caused by natural and environmental hazards [66,72]. In this study, digital elevation model (DEM) data at 30-m spatial resolution were derived from USGS National Elevation Dataset for the year 2018. The mean elevation of each county (in meter) was calculated in ArcGIS.

- Other data.

As mentioned earlier, GDP per capita indicates an area's economic vulnerability to disasters and generally, higher per capita GDP corresponds to lower impacts from environmental disasters. In this research, county GDP amounts (U.S. dollars) were obtained from the Bureau of Economic Analysis, U.S. Department of Commerce website for the year 2018. The county GDP value was divided by the total county population in 2018 to calculate the per capita GDP of each county. The county total population and population density data were obtained from U.S. Census Bureau website. High population density usually corresponds to higher damage from disasters in an area. Finally, TC frequency data were obtained from the SHEL DUS website. SHEL DUS reports the number of occasions a county has been hit by a disaster (TC in this research) for a given time period along with the monetary damage (U.S. dollars) sustained by that county. The total amount of damage for each county from TCs between 1996 and 2018 was later adjusted to the 2018 inflation rate to be constant with the datasets used in this research.

2.3. Data Analyses

After obtaining the data for all the variables, the data were transformed and normalized. In this study, transformation refers to the conversion of the raw variables into averages or percentages where necessary. As a result, the different sizes and characteristics of inland counties can be compared. After data transformation, they were normalized so that all the data can be compared based on the same reference points. In this paper, we used the max–min approach to normalize the data for the factors of TC-related damage. Since the measuring units of different factors used in this research are different, normalizing the

data into the same measuring range (from 0 to 1) was warranted. The max–min approach was used to normalize each factor using the below equation [37]:

$$x'_i = (x_i - x_{\min}) / (x_{\max} - x_{\min}) \quad (1)$$

where x'_i is the normalized value of the i th cell of factor x , x_i is the value of i th cell of factor x , x_{\max} is the maximum value of factor x , and x_{\min} is the minimum value of factor x . After normalization, the value of each factor ranges from 0 (the lowest value) to 1 (the highest value).

After the data preprocessing, multicollinearity between the seven selected factors was tested using the Tolerance and Variance Inflation Factors (VIF) in a correlation matrix. Tolerance values closer to 1 and greater than 0 and VIF values greater than 1 and smaller than 4 are considered low degrees of multicollinearity [73]. Factors with a high degree of multicollinearity were excluded from the analysis.

Per capita property damage in each county caused by the TCs between 1996 and 2018 was mapped to explore the spatial distribution of damages across the study area. Additionally, all the transformed factors with low multicollinearity were also mapped to visualize their spatial distribution as well as potential hotspots in the study area. Furthermore, Global Moran's I statistic was also calculated to check for spatial autocorrelation in the damage variable [66]. The Global Moran's I statistic can be calculated using the below equation [68]:

$$\text{Global Moran's } I = \frac{N}{\sum_{i=1}^N \sum_{j=1}^N W_{ij}} \times \frac{\sum_{i=1}^N \sum_{j=1}^N W_{ij} (X_i - \bar{X})(X_j - \bar{X})}{\sum_{i=1}^N (X_i - \bar{X})^2} \quad (2)$$

where N is the number of spatial units (counties in this study). W_{ij} represents the spatial weight matrix. X_i and X_j are the values of variables and \bar{X} is the mean.

The main objectives of this research were to understand the intersection of different dimensional factors of TC-related damage at the county-level and how these factors influence property damage caused by TCs spatially. The GWR model was used to explore the spatial variation in the relationship between TC property damage and selected factors. The GWR model can be explained using the following equations [68,74]:

$$y_i(u) = \beta_{0i}(u) + \beta_{1i}(u)X_{1i} + \beta_{2i}(u)X_{2i} + \dots + \beta_{ai}(u)X_{ai} \quad (3)$$

$$\beta_{ai}(u) = (X^t W(u) X)^{-1} X^t W(u) y \quad (4)$$

$$W_n(u) = e^{-0.5 \left(\frac{d_n(u)}{b} \right)^2} \quad (5)$$

where X_{ai} are the dependent variables, and $\beta_{ai}(u)$ is the coefficient. The coefficient is calculated by the matrix of independent variables (X_{ai}) and weight matrix at location u . $W(u)$ is the weight matrix calculated by $W_n(u)$. The distance between n th observation and location u is calculated by $d_n(u)$ where b is the kernel radius.

However, a global regression model, Ordinary Least Squares (OLS), was also used and compared to the GWR results. The dependent variable, log converted per capita property damage caused by landfalling TCs, was regressed against the independent variables and selected factors of TC-related damages in both OLS and GWR models. While the OLS model considers the relationship between variables as constant, GWR shows the spatial variations among the dependent and independent variables and explores their relationship in geographic locations. Additionally, GWR offers coefficients for all the independent variables separately [69], whereas OLS only provides an overall influence of independent variables over the dependent variable. The corrected Akaike information criterion (AICc) was used to assess the model fitness for OLS and GWR. Since the AICc reflects the difference between the observed and predicted values, a lower AICc value corresponds to the better model fit.

3. Results

3.1. Spatial Patterns of Property Damage and Influential Factors

There are 170 inland counties and parishes in this study: 61 in Alabama, 37 in Louisiana, and 72 in Mississippi. There was over USD 4.46 billion of property damage (adjusted to the 2018 inflation rate) caused by landfalling TCs (excluding Hurricane Katrina) in these inland areas between 1996 and 2018. The average damage per county was over USD 26 million during this period. The average per capita property damage in the study area was USD 1135.58. The per capita property damage was classified into six categories, including no damage, very low, low, moderate, high, and very high for visualization purposes (Figure 2).

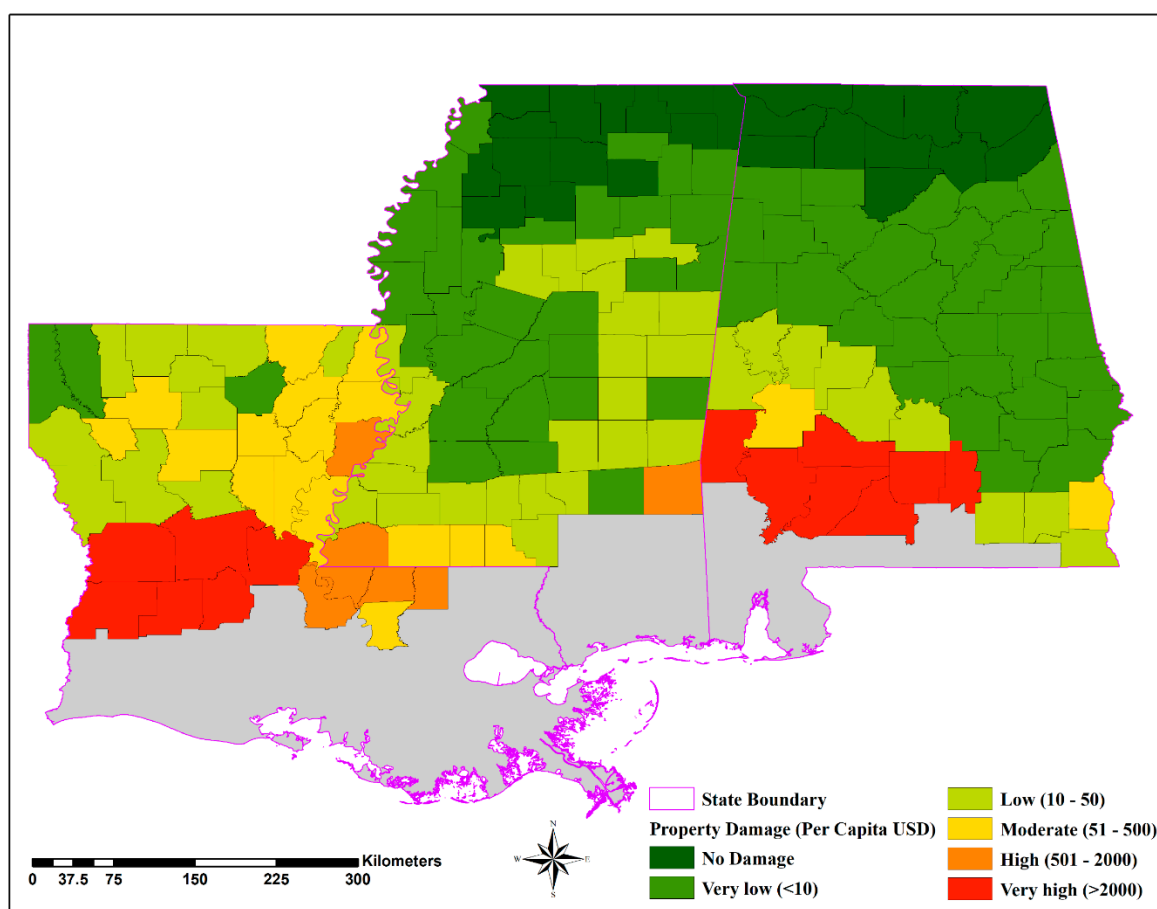


Figure 2. Per capita property damage spatial distribution in the inland counties.

Regionally, the southern part of the study area sustained higher per capita damage compared to the northern part. In particular, the southwestern Alabama and Louisiana region had the highest per capita damage (>USD 2000) and counties in inland Mississippi had the lowest average per capita damages (Figure 2). Inland counties in Alabama had the highest average property damages (USD 2134.85 average per capita damage) followed by inland counties in Louisiana (USD 1617.12 average per capita damage). In fact, 7 out of the 10 highest per capita damages sustained by the counties during the study period are in Alabama and 3 of them are in Louisiana. Inland counties in Mississippi had mostly very low-moderate level of per capita damages (>USD 50) with a few exceptions (some southern counties in this state had moderate-high per capita damages). A total of 25 counties in the study area had no damages reported during 1996–2018, located in northern Alabama and Mississippi.

As discussed earlier, TC-related property damages are influenced by many factors, including the seven factors selected in this study. Therefore, examining the spatial distributions of these factors will explore geographic trends in the datasets. However, population density was excluded from the list of factors due to the high multicollinearity ($VIF > 7$). Thus, our final six factors include TC frequency, total rainfall (meters), per capita GDP (USD), total wind speed (knots), county mean elevation (meters), and county social vulnerability percentile (Figure 3). The spatial distributions of these factors were manually classified for visualization purpose. Higher values for TC frequency were found around the southern part of the study area (Figure 3a). These counties experienced at least five TCs during the study period. Jones County, Mississippi had the highest TC frequency of nine in the study area. The lower values of TC frequency are concentrated around the northern part of the study area. The central part of the tri-state region experienced low-moderate TC frequency (between two and four). Similar to the TC frequency, higher values of county total rainfall and wind speed are concentrated along the southern part and lower values are concentrated along the northern part of the study area (Figure 3b,d, respectively). As storms decay inland with an increasing pressure field and weaker pressure gradient, storm rainfall can become disassociated from the central core [75]. However, there are some variations in total county rainfall and wind speed among the three states. For example, inland Alabama counties had the highest total TC rainfall amount on average (1.65 m per county) followed by Mississippi (1.36 m per county). Inland Louisiana had the lowest total county TC rainfall on average (0.81 m per county). Inland counties in Louisiana had the highest county wind speed on average (191.55 knots per county). Inland counties in Alabama and Mississippi had similar county TC wind speeds on average (138.17 and 131.23 knots per county, respectively).

The pattern is completely the opposite when it comes to the mean elevation of the county (Figure 3e). Lower values of county mean elevation are concentrated along the southern part of the study area. Northern Alabama counties have a higher mean elevation compared to the other counties. The lowest mean elevation was found in Pointe Coupee Parish, Louisiana (13.83 m), and the highest mean elevation was found in DeKalb County, Alabama (381.59 m). There are no definite patterns of high and low values of per capita GDP (USD) found in the study area (Figure 3c). Almost 96% of the inland counties had per capita GDP less than the national average in 2018 (USD 62,794.60), and 60% of the inland counties had per capita GDP less than USD 30,000 in 2018. Similar to the GDP, no pattern of high and low county SoVI percentile scores were found in the study area. However, around 44% of the counties had SoVI score above the 60th percentile and 22% of the counties had a SoVI score above the 80th percentile, which are considered highly socially vulnerable counties to natural disasters (Figure 3f). Only 12% of the total 170 inland counties had a SoVI score below the 20th percentile.

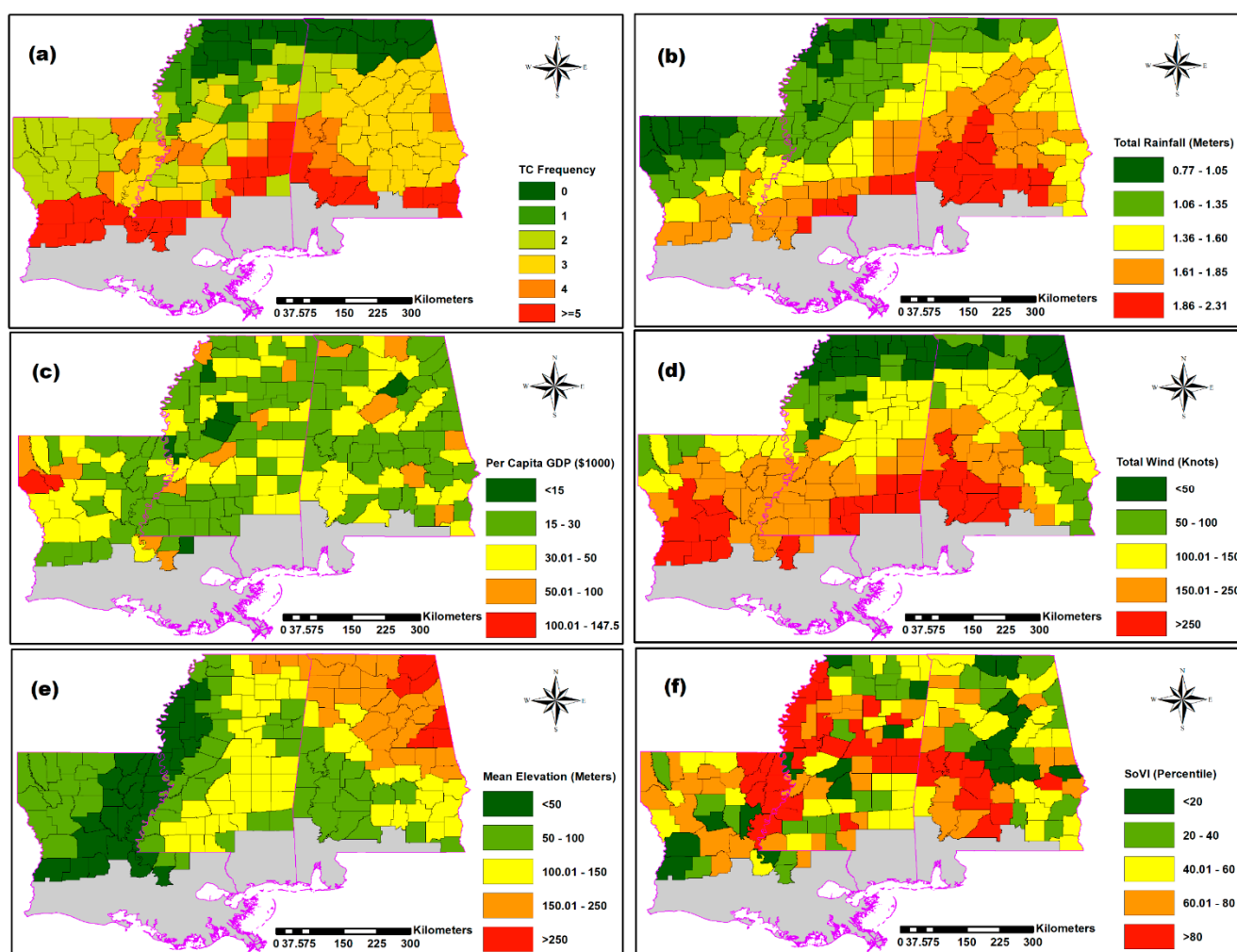


Figure 3. Spatial patterns and distributions of six factors: (a) TC frequency; (b) total TC rainfall (m); (c) county per capita GDP; (d) total TC wind (knots); (e) county mean elevation (m); and (f) county SoVI percentile.

3.2. Influential Factors on Property Damage

Since TC-related property damage is influenced by a wide variety of factors, we selected six different factors to assess their influences on TC property damage at the county level in the inland areas. However, not all the factors influence TC property damage in the same way. For example, hazards associated with TCs, such as rainfall and wind, increase the TC vulnerability in an area. However, economic development of a county, such as per capita GDP, helps the community to decrease the impacts of TCs.

To examine the degree and direction of influence that the six selected factors might have on TC-related property damage in inland areas, we conducted both OLS and GWR regression analyses. Before doing the OLS and GWR, we analyzed the spatial pattern of the TC-related property damage in the study area using the spatial autocorrelation (Moran's I) in ArcGIS. A statistically significant ($p < 0.01$) Moran's I score of 0.28 with z-score of 5.56 suggests that TC-related property damage is not equally distributed across the inland counties and there is a presence of a spatial autocorrelation problem in the damage values. Thus, the relationship between the dependent and explanatory variables would be better explained by employing a GWR model, as GWR is capable of modeling the spatial variations of the data. Since GWR provides individual coefficients of each independent variable for all counties compared to OLS, which only shows the overall influence of independent variables on dependent variables, it can reveal the local characteristics of each county and minimize the spatial autocorrelation problem [66]. Table 1 illustrates the

coefficient values for the OLS model and average coefficient values and standard deviation for all the inland counties of the GWR model.

Table 1. Influence of six selected factors on TC-related property damage in inland counties using OLS and GWR models.

	Coefficient (OLS)		Coefficient (GWR)	
	(β)	Standard Deviation	Average (Mean β)	Standard Deviation
Constant	0.16	–	–0.15	1.15
TC frequency	0.99 **	0.21	1.25	1.16
TC rainfall	0.82 *	0.21	1.51	1.47
TC wind	1.97 ***	0.22	1.09	0.65
Mean elevation	–1.64 ***	0.19	–1.57	1.61
County SoVI	0.15	0.27	0.26	0.29
Per capita GDP	–0.12	0.15	–0.46	0.51
R-square		0.61		0.82
Adjusted R-square		0.6		0.77
AICc		382.49		310.18
Global Moran's I of Residuals		0.34 ***		0.1 **

*** $p < 0.01$ level, ** $p < 0.05$ level, * $p < 0.1$ level.

3.2.1. OLS Results

The influence of the selected factors on TC-related property damage was first examined using OLS. Table 1 shows that there are statistically significant relationships between the explanatory factors and the dependent variable. The OLS model explains over 60% ($R^2 = 0.61$) of the variance by regressing six explanatory factors against the dependent variable (TC-related property damage). Four of the six explanatory factors were statistically significant in the OLS model with different directions.

In the OLS model, county TC wind speed had the highest influence on property damage with a positive direction. Therefore, a unit increase in the county TC wind speed would increase the TC-related property damage by almost 200% ($\beta = 1.97$; $p < 0.01$) in the study area. County TC rainfall had a weaker relationship with property damage in the inland areas than wind in the OLS model, as one-unit increase in county total rainfall would increase property damage by 82% (Table 1). Previous research found that wind had a weaker influence on TC-related losses in the inland areas than rain since TC wind tends to decay as the storms move inland [45]. However, this research suggests that TC wind still plays a major role in causing property losses in inland areas. As expected, the mean elevation of a county had a strong negative impact on property damage in the study area as shown in Table 1. A unit increase in elevation would decrease the property damage by 164%. This result is consistent with previous studies [66,72] as low-lying inland areas are subject to TC freshwater flooding due to heavy rainfall and therefore sustain property damages as found in this study. Additionally, TC frequency also had a strong positive relationship with TC-related property damage. A unit increase in TC frequency would increase the property damage by almost 100% in the study area. This result corroborates the fact that areas that are more frequently impacted by TCs sustain higher property damages. Interestingly, county social vulnerability and per capita GDP had no statistically significant relationship with property damage even though SoVI had a positive relationship and per capita GDP had a negative relationship with property damage as expected.

3.2.2. GWR Results

All the factors that had strong relationships with property damage in the OLS model also strongly influenced property damage in the GWR model as shown in Table 1. Since the GWR considers the local differences, substantial improvement in explaining the variance (from 61% in the OLS model to 82%) was found in the GWR model. All the six factors significantly influence the TC-related property damage in the inland counties in the study area. In the GWR model, county TC rainfall and mean elevation were found as the most

influential factors. A one-unit increase in the rainfall and one-unit decrease in mean elevation would increase the property damage by over 150% on average across the study area (Table 1). County TC wind speed also significantly influences property damage caused by TCs, as a one-unit increase in county TC wind speed would increase the property damage value by 109% on average. TC frequency is another influential factor of county property damage value, as a one-unit increase in TC frequency would increase average property damage by 125% in the inland counties. Per capita GDP and county SoVI have comparatively lower influences on property damage, as a one-unit decrease in per capita GDP and a one-unit increase in county SoVI would increase the average property damage in inland counties by 46% and 26%, respectively. A higher R^2 value in the GWR model suggests that there might be a presence of spatial non-stationarity between the dependent and independent variables as shown in the previous study [74]. Since GWR considers the geographical locations and variations in the dataset, the degree of influence of the six independent factors varies spatially. The local coefficients of the six independent factors are mapped (Figure 4) to visualize the spatially varying relationships between property damage and the six explanatory variables. Figure 4 shows the spatial distributions of the coefficients of the six independent factors (classified manually for visualization purpose) in the GWR model. The spatial patterns of the coefficient distribution further suggest that the relationship between TC-related property damage and the six influential factors are not constant in the inland counties of the study area. For example, western Louisiana has higher coefficients of TC frequency and comparatively lower TC rainfall coefficients (Figure 4a,b, respectively) which suggests that the former has a larger impact on property damage in this region than the latter. Southern counties in inland Alabama and Mississippi had the highest TC rainfall coefficients compared to northern counties in these two states. This suggests that TC rainfall impacts are much more severe in the southern region of these two states, and it decreases as TCs move farther inland (Figure 4b). Counties in the central and southeastern part of inland Alabama have the highest coefficients for TC wind, suggesting that property damages in these counties are also significantly influenced by TC wind (Figure 4d). Lower coefficients of mean elevation are concentrated along the southwestern Mississippi and eastern Louisiana region, which indicates that TC-related property damage in this part is largely influenced by lower elevation (Figure 4e). SoVI has very little influence on property damage in Louisiana as shown by lower SoVI coefficients in this state, which is the opposite in the case of Alabama (Figure 4f). Most of the counties with negative per capita GDP coefficients suggest that this factor influences property damage across the entire study area (Figure 4c).

3.2.3. OLS and GWR Model Comparison

Table 1 shows the R^2 and AICc values of OLS and GWR models. With an R^2 value of 0.82 and AICc value of 310.18, GWR has the higher R^2 value and lower AICc value than OLS ($R^2 = 0.61$; AICc = 382.49). These results suggest that the GWR model performs better than the OLS. With a higher R^2 value, GWR portrays a better relationship between the dependent and independent variables than OLS. The lower AICc value in the GWR model indicates that GWR models a closer approximation of the real-world scenario and a better model fit than OLS with the datasets used.

Nevertheless, the R^2 and AICc values are only the measurement about the overall model performance. We also measured the spatial autocorrelation (Global Moran's I) of the residuals in both models to check the spatial non-stationarity (Table 1). As shown in Table 1, residuals in the OLS model have a statistically significant Global Moran's I value of 0.34. However, the Global Moran's I value of the residuals in the GWR model significantly decreased to only 0.1. Therefore, residual independence is violated in the OLS model.

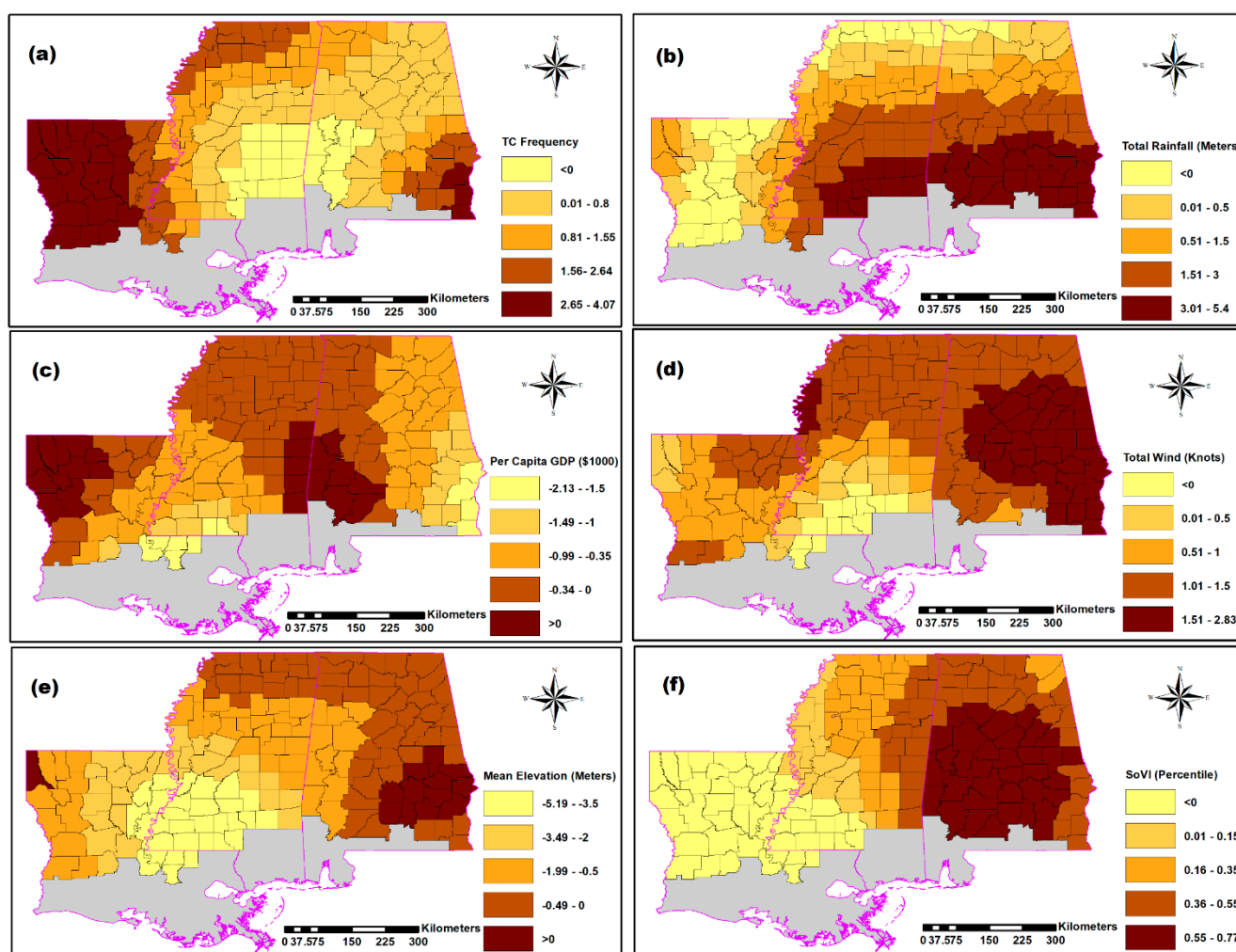


Figure 4. Spatial distributions of coefficients of the six independent variables in the GWR model: (a) TC frequency; (b) TC rainfall; (c) per capita GDP; (d) TC wind; (e) mean elevation; and (f) county SoVI percentile.

4. Discussion

After landfall, TCs frequently tend to weaken due to a number of factors, including loss of latent heat, augmented friction, temperature gradients, wind shear, and dry air intrusion [76]. Consequently, previous studies focused on coastal areas or landfall zones to measure the impacts of TCs. However, TCs maintaining or even increasing strength farther inland have been well documented [6,77,78]. Therefore, inland losses due to landfalling TCs could be substantial as shown in this study.

As mentioned earlier, meteorological storm characteristics, especially wind, rainfall, and tornadoes, are the main hazards associated with TCs that cause property damage and fatalities. Accordingly, previous studies mainly analyzed the impacts of these storm characteristics to explain losses due to TCs. However, research shows that other than the meteorological characteristics of a storm, other factors, such as socio-economic vulnerability and physical characteristics, such as elevation, could also influence losses due to disasters, including TCs [28,42,66]. Therefore, this study took a unique approach to understand the intersection of meteorological storm characteristics, socioeconomic vulnerability, and physical characteristics of the study area for a combined influence on property damage.

Among the different meteorological characteristics of TCs, previous studies found that inland flooding due to heavy rainfall was the main factor that influenced TC losses while impacts of TC wind were minimal [25,44,45]. However, findings from this study show that high winds associated with landfalling TCs have significant impacts on TC property

damage in the study area (Table 1). Rapid intensification of TCs before landfall and TCs that maintain strengths for a longer period after landfall might be one possible explanation for this result. In the past three years, the Gulf of Mexico region has seen three storms rapidly intensify before landfall. Of these, only Hurricane Laura in 2020 affected the tristate study region. Estimated damage and physical storm variables aggregated at the county level from Hurricane Laura are preliminary and are, therefore, not included in this analysis. Even though hurricane force winds are very rare in inland areas (very few inland counties had hurricane force wind in this research during the study period), rapid intensification of hurricanes in this region and hurricanes that maintain intensity for a longer period of time (Hurricane Michael in 2018 and Hurricane Laura in 2020, for example) will cause higher property damage if these types of storms become more common in the future. Apart from TC wind, we also found that rainfall associated with TCs also impacted property damage in the study area substantially, which is consistent with previous studies. Since most counties of the study area had no TC-induced tornadoes during the study period, we did not consider tornadoes as a contributing factor to property damage in this study. Most TC tornadoes are brief with intensities less than EF2, thus damage from TC tornadoes is minimal unless a densely populated area is impacted. In addition, elevation had a strong negative relationship with property damage on both OLS and GWR model, suggesting that counties with higher elevation sustained less property damage. Previous studies also support our findings that higher elevation plays a significant role in preventing TC-induced flooding and resulting property damage [66,79].

As expected, we found that SoVI had a positive relationship and per capita GDP had a negative relationship with property damage (Table 1). However, they lost their statistical significance when a multivariate approach (OLS model) was taken. Nevertheless, the GWR results show that majority of the counties had high positive SoVI coefficients (Figure 4f) and high negative per capita GDP coefficients (Figure 4c), further confirming their overall signifying impacts on TC property damage in the study area.

The findings from the GWR results could be beneficial to weather forecasters, local emergency managers (EMs), and policy makers in terms of disaster preparedness and mitigation plans in the U.S. and globally. This research has once again proven that inland precipitation and heavy flooding continues to be a leading cause of property damage. Recent U.S. TCs, such as Hurricane Harvey 2017 and Hurricane Florence 2018, stalled or barely moved between the coastal and inland zones, creating widespread destructive flooding that surprised people. Forecasters and EMs should continue to make progress in specific messaging for TCs that are slow-moving inland rain producers. These types of flooding storms may become more common globally [80] and in this region in the future [81]. However, other studies find a projected increase in TC translational speed globally [82] and in this region [83], which would indicate greater odds of storms maintaining high winds farther inland. The widespread inland destruction from Hurricanes Michael 2018 and Laura 2020 also surprised inland residents who had never witnessed inland winds of that intensity in their lifetimes. Specific targeted messaging should also be used to emphasize either fast-moving or strong storms that do not experience inland decay at the normal rate so that inland residents can be more aware of potential damage. EMs could detect specific areas in need of improvements to minimize the impacts of TCs (e.g., property damage). As the GWR model accounts for the spatially varying relationships between the dependent and independent variables, policies based on the GWR would result in a more effective disaster management plan by reflecting local conditions than a 'one-size-fits-all' disaster management plan. EMs and policymakers could make area-specific plans for emergencies as GWR provides evidence to make decisions in their local communities.

Despite some unique strengths to this study, there were some limitations. Firstly, a smaller geographic unit, such as census-tract or block group, could provide more detailed information in explaining the impacts of different factors used in this study on property damage. However, TC damage data are not available at a finer spatial scale than county-level for the study area, and therefore, we had to choose counties as our spatial unit

in this study. Secondly, some other key factors could be used in future studies, which might produce better results. For example, studies found that soil moisture could be an important factor for TC reintensification [6], which could be used as an explaining factor for TC damage in future studies. Thirdly, SoVI was used in this study to measure the impacts of overall social vulnerability on TC damage. However, using individual social vulnerability variables (SoVI is constructed from 29 individual variables) as factors to explain property damage might produce different results. Additionally, the SoVI used in this research was for the year 2014. A more recent social vulnerability index could also produce better results. Finally, some identified factors, such as elevation, wind, and rainfall, are continuous geographic phenomena which were aggregated at the county scale for the purpose of this study, and thus might have influenced the results. However, if data become available, future studies should consider census tracts or blocks to analyze factors impacting TC damage in this region and thus minimize this influence.

5. Conclusions

Previous research on TC impacts in inland areas were limited to areas that are adjacent to coastal areas where impacts were the highest. However, TC impacts can be extensive farther inland. Therefore, we included all the counties that fall into the defined inland zone in this study. Factors from different dimensions (e.g., meteorological storm characteristics, socioeconomic vulnerability and physical characteristics of areas impacted) were assessed to measure their impacts on TC damage. Results show that storm characteristics, such as wind, rainfall, and TC frequency, all had significant impacts on property damage in the study area. Furthermore, findings of this research suggest that the factors used in this study to assess the influence on TC-related property damage vary across space. The GWR model was found to be the better fit of the data used in this research and better explained the variance in the dependent variable than OLS. TC wind was found as one of the major contributing factors to property damage in the study area in both OLS and GWR models, which appears to contradict previous research where freshwater flooding from heavy rain associated with TCs is the main factor behind TC impacts in the inland areas. County mean elevation was found as another important factor that needs to be considered while assessing the property damage caused by TCs. Additionally, a direct relationship was found between TC frequency and property damage in the study area. Despite many counties being characterized by high social vulnerability, it was found that the impacts of social vulnerability on property damage were lower than the other factors used in this research. Perhaps this can be explained by the low per capita GDP in the study area, especially the counties characterized by high social vulnerability.

The findings of this research are beneficial to policymakers and emergency managers. The results help to explain the intersection between meteorological storm characteristics, physical characteristics of the area impacted, and socioeconomic vulnerability to disasters on the associated impacts from TCs in the inland areas. Additionally, the findings of this study shed light on the importance of considering spatially varying relationships between property damage and the explanatory factors. This research provides helpful estimates for initiating a discussion on investments in mitigation and preparedness actions ahead of the inevitable future inland storms with potential to cause massive property damage. Forecasters and emergency managers should continue to strengthen their targeted messaging efforts for inland TCs that are either prolific rain and flooding producers or strong inland wind damage storms. This is especially true for counties with lower elevations and higher SoVI scores.

Overall, this study empirically documented that inland areas can be substantially impacted by landfalling TCs and the factors that influence the inland TC impacts. Methods and approaches taken in this study could be applied to other inland areas globally to explore major factors that influence TC impacts. Future studies should consider additional factors (e.g., soil moisture and TC intensity) at a finer spatial scale (possibly at census tract or block group level) to minimize inland TC impacts.

Author Contributions: Conceptualization, Shaikh Abdullah Al Rifat, Jason C. Senkbeil and Weibo Liu; methodology, Shaikh Abdullah Al Rifat, Weibo Liu and Jason C. Senkbeil; formal analysis, Shaikh Abdullah Al Rifat, Jason C. Senkbeil and Weibo Liu; writing—original draft preparation, Shaikh Abdullah Al Rifat; writing—review and editing, Jason C. Senkbeil and Weibo Liu; All authors have read and agreed to the published version of the manuscript.

Funding: This research received no external funding.

Institutional Review Board Statement: Not applicable.

Informed Consent Statement: Not applicable.

Data Availability Statement: The data used in this study are openly available in NOAA's International Best Track Archive for Climate Stewardship (IBTrACS) (<https://www.ncdc.noaa.gov/ibtracs/index.php?name=ib-v4-access>), Parameter-elevation Regressions on Independent Slopes Model (PRISM) Climate Group (<https://prism.oregonstate.edu/>), Hazards and Vulnerability Research Institute at University of South Carolina (<http://artsandsciences.sc.edu/geog/hvri/sovi%C2%AE-0>), USGS National Elevation Dataset (<https://catalog.data.gov/dataset/usgs-national-elevation-dataset-ned>), Bureau of Economic Analysis, US Department of Commerce (<https://www.bea.gov/>), U.S. Census Bureau (<https://www.census.gov/en.html>), and Spatial Hazard Events and Losses Database for the U.S. (SHELDUS) (<https://cemhs.asu.edu/sheldus>).

Acknowledgments: We would like to thank the three anonymous reviewers and editors for providing valuable comments and suggestions which helped improve the manuscript greatly.

Conflicts of Interest: The authors declare no conflict of interest.

References

- Peduzzi, P.; Chatenoux, B.; Dao, H.; De Bono, A.; Herold, C.; Kossin, J.; Mouton, F.; Nordbeck, O. Global trends in tropical cyclone risk. *Nat. Clim. Chang.* **2012**, *2*, 289–294. [CrossRef]
- Bakkensen, L.A.; Mendelsohn, R.O. Risk and adaptation: Evidence from global hurricane damages and fatalities. *J. Assoc. Environ. Resour. Econ.* **2016**, *3*, 555–587. [CrossRef]
- Bakkensen, L.A.; Shi, X.; Zurita, B.D. The impact of disaster data on estimating damage determinants and climate costs. *Econ. Disasters Clim. Chang.* **2018**, *2*, 49–71. [CrossRef]
- Narita, D.; Tol, R.S.J.; Anthoff, D. Damage costs of climate change through intensification of tropical cyclone activities: An application of FUND. *Clim. Res.* **2009**, *39*, 87–97. [CrossRef]
- Ranson, M.; Kousky, C.; Ruth, M.; Jantarasami, L.; Crimmins, A.; Tarquinio, L. Tropical and extratropical cyclone damages under climate change. *Clim. Chang.* **2014**, *127*, 227–241. [CrossRef]
- Arndt, D.S.; Basara, J.B.; McPherson, R.A.; Illston, B.G.; McManus, G.D.; Demko, D.B. Observations of the overland reintensification of Tropical Storm Erin. *Bull. Am. Meteorol. Soc.* **2009**, *90*, 1079–1094. [CrossRef]
- Chang, H.; Niyogi, D.; Kumar, A.; Kishtawal, C.M.; Dudhia, J.; Chen, F.; Mohanty, U.C.; Shepherd, M. Possible relation between land surface feedback and the post-landfall structure of monsoon depressions. *Geophys. Res. Lett.* **2009**, *36*. [CrossRef]
- Lian-Shou, C. Research progress on the structure and intensity change for the landfalling tropical cyclones. *J. Trop. Meteorol.* **2012**, *18*, 113.
- Emanuel, K.; Callaghan, J.; Otto, P. A hypothesis for the redevelopment of warm-core cyclones over northern Australia. *Mon. Weather Rev.* **2008**, *136*, 3863–3872. [CrossRef]
- Ye, M.; Wu, J.; Liu, W.; He, X.; Wang, C. Dependence of tropical cyclone damage on maximum wind speed and socioeconomic factors. *Environ. Res. Lett.* **2020**, *15*. [CrossRef]
- Pielke, R.A., Jr. Future economic damage from tropical cyclones: Sensitivities to societal and climate changes. *Philos. Trans. R. Soc. A Math. Phys. Eng. Sci.* **2007**, *365*, 2717–2729. [CrossRef] [PubMed]
- Pielke, R.A., Jr.; Gratz, J.; Landsea, C.W.; Collins, D.; Saunders, M.A.; Musulin, R. Normalized hurricane damage in the United States: 1900–2005. *Nat. Hazards Rev.* **2008**, *9*, 29–42. [CrossRef]
- Burton, C.G. Social vulnerability and hurricane impact modeling. *Nat. Hazards Rev.* **2010**, *11*, 58–68. [CrossRef]
- Senkbeil, J.C.; Brommer, D.M.; Comstock, I.J. Tropical cyclone hazards in the USA. *Geogr. Compass* **2011**, *5*, 544–563. [CrossRef]
- Mendelsohn, R.; Emanuel, K.; Chonabayashi, S.; Bakkensen, L. The impact of climate change on global tropical cyclone damage. *Nat. Clim. Chang.* **2012**, *2*, 205–209. [CrossRef]
- Weinkle, J.; Landsea, C.; Collins, D.; Musulin, R.; Crompton, R.P.; Klotzbach, P.J.; Pielke, R. Normalized hurricane damage in the continental United States 1900–2017. *Nat. Sustain.* **2018**, *1*, 808–813. [CrossRef]
- Knabb, R.; Rhome, J.; Brown, D. *National Hurricane Center. Tropical Cyclone Report: Hurricane Katrina, 23–30 August 2005. National Oceanic and Atmospheric Administration; National Weather Service, National Hurricane Center: Miami, FL, USA, 2005.*
- Blake, E.S.; Landsea, C.; Gibney, E.J. *The Deadliest, Costliest, and Most Intense United States Tropical Cyclones from 1851 to 2010 (and Other Frequently Requested Hurricane Facts); NOAA Technical Memorandum NWS NHC: Washington, DC, USA, 2011.*

19. Benfield, A. *Weather, Climate and Catastrophe Insight: 2017 Annual Report*; London Aon: London, UK, 2018; p. 56.
20. Mestre, O.; Hallegatte, S. Predictors of tropical cyclone numbers and extreme hurricane intensities over the North Atlantic using generalized additive and linear models. *J. Clim.* **2009**, *22*, 633–648. [\[CrossRef\]](#)
21. Anderson, W.F.; Maaß, A.; Ozias-Akins, P. Genetic Variability of a Forage Bermudagrass Core Collection. *Crop. Sci.* **2009**, *49*, 1347–1358. [\[CrossRef\]](#)
22. Zhou, X.; Liu, Z.; Yan, Q.; Zhang, X.; Yi, L.; Yang, W.; Xiang, R.; He, Y.; Hu, B.; Liu, Y.; et al. Enhanced Tropical Cyclone Intensity in the Western North Pacific During Warm Periods Over the Last Two Millennia. *Geophys. Res. Lett.* **2019**, *46*, 9145–9153. [\[CrossRef\]](#)
23. Senkbeil, J.C.; Sheridan, S.C. A postlandfall hurricane classification system for the United States. *J. Coast. Res.* **2006**, *22*, 1025–1034. [\[CrossRef\]](#)
24. Kovach, M.M.; Konrad, C.E. The spatial distribution of tornadoes and high wind impacts associated with inland-moving tropical cyclones in the southeastern United States. *Phys. Geogr.* **2014**, *35*, 245–271. [\[CrossRef\]](#)
25. Rappaport, E.N. Loss of life in the United States associated with recent Atlantic tropical cyclones. *Bull. Am. Meteorol. Soc.* **2000**, *81*, 2065–2074. [\[CrossRef\]](#)
26. Cutter, S.L.; Mitchell, J.T.; Scott, M.S. Revealing the vulnerability of people and places: A case study of Georgetown County, South Carolina. *Ann. Assoc. Am. Geogr.* **2000**, *90*, 713–737. [\[CrossRef\]](#)
27. Tierney, K.J.; Lindell, M.K.; Perry, R.W. *Facing the Unexpected: Disaster Preparedness and Response in the United States*; Joseph Henry Press: Washington, DC, USA, 2002.
28. Cutter, S.L.; Boruff, B.J.; Shirley, W.L. Social vulnerability to environmental hazards. *Soc. Sci. Q.* **2003**, *84*, 242–261. [\[CrossRef\]](#)
29. Emrich, C.T.; Cutter, S.L. Social vulnerability to climate-sensitive hazards in the Southern United States. *Weather Clim. Soc.* **2011**, *3*, 193–208. [\[CrossRef\]](#)
30. Flanagan, B.E.; Gregory, E.W.; Hallisey, E.J.; Heitgerd, J.L.; Lewis, B. A social vulnerability index for disaster management. *J. Homel. Secur. Emerg. Manag.* **2011**, *8*. [\[CrossRef\]](#)
31. Hossain, M.K.; Meng, Q. A thematic mapping method to assess and analyze potential urban hazards and risks caused by flooding. *Comput. Environ. Urban. Syst.* **2020**, *79*, 101417. [\[CrossRef\]](#)
32. Hossain, M.K.; Meng, Q. A multi-decadal spatial analysis of demographic vulnerability to urban flood: A case study of Birmingham City, USA. *Sustainability* **2020**, *12*, 9139. [\[CrossRef\]](#)
33. Ashley, W.S.; Strader, S.; Rosencrants, T.; Kremenec, A.J. Spatiotemporal changes in tornado hazard exposure: The case of the expanding bull’s-eye effect in Chicago, Illinois. *Weather Clim. Soc.* **2014**, *6*, 175–193. [\[CrossRef\]](#)
34. Strader, S.M.; Ashley, W.S. The expanding bull’s-eye effect. *Weatherwise* **2015**, *68*, 23–29. [\[CrossRef\]](#)
35. Freeman, A.C.; Ashley, W.S. Changes in the US hurricane disaster landscape: The relationship between risk and exposure. *Nat. Hazards* **2017**, *88*, 659–682. [\[CrossRef\]](#)
36. Bierwagen, B.G.; Theobald, D.M.; Pyke, C.R.; Choate, A.; Groth, P.; Thomas, J.V.; Morefield, P. National housing and impervious surface scenarios for integrated climate impact assessments. *Proc. Natl. Acad. Sci. USA* **2010**, *107*, 20887–20892. [\[CrossRef\]](#) [\[PubMed\]](#)
37. Rifat, S.A.A.; Liu, W. Quantifying Spatiotemporal Patterns and Major Explanatory Factors of Urban Expansion in Miami Metropolitan Area During 1992–2016. *Remote Sens.* **2019**, *11*, 2493. [\[CrossRef\]](#)
38. Rijal, S.; Rimal, B.; Sloan, S. Flood hazard mapping of a rapidly urbanizing city in the foothills (Birendranagar, Surkhet) of Nepal. *Land* **2018**, *7*, 60. [\[CrossRef\]](#)
39. Schmidt, S.; Kemfert, C.; Höppe, P. The impact of socio-economics and climate change on tropical cyclone losses in the USA. *Reg. Environ. Chang.* **2010**, *10*, 13–26. [\[CrossRef\]](#)
40. Wen, S.; Wang, Y.; Su, B.; Gao, C.; Chen, X.; Jiang, T.; Tao, H.; Fischer, T.; Wang, G.; Zhai, J. Estimation of economic losses from tropical cyclones in China at 1.5 °C and 2.0 °C warming using the regional climate model COSMO-CLM. *Int. J. Climatol.* **2019**, *39*, 724–737. [\[CrossRef\]](#)
41. Hallegatte, S. A normative exploration of the link between development, economic growth, and natural risk. *Econ. Disasters Clim. Chang.* **2017**, *1*, 5–31. [\[CrossRef\]](#)
42. Wu, J.; Han, G.; Zhou, H.; Li, N. Economic development and declining vulnerability to climate-related disasters in China. *Environ. Res. Lett.* **2018**, *13*, 34013. [\[CrossRef\]](#)
43. Wu, J.; Li, Y.; Li, N.; Shi, P. Development of an asset value map for disaster risk assessment in China by spatial disaggregation using ancillary remote sensing data. *Risk Anal.* **2018**, *38*, 17–30. [\[CrossRef\]](#)
44. Czajkowski, J.; Kennedy, E. Fatal tradeoff? Toward a better understanding of the costs of not evacuating from a hurricane in landfall counties. *Popul. Environ.* **2010**, *31*, 121–149. [\[CrossRef\]](#)
45. Czajkowski, J.; Simmons, K.; Sutter, D. An analysis of coastal and inland fatalities in landfalling US hurricanes. *Nat. Hazards* **2011**, *59*, 1513–1531. [\[CrossRef\]](#)
46. Schmidlin, T.W. Human fatalities from wind-related tree failures in the United States, 1995–2007. *Nat. Hazards* **2009**, *50*, 13–25. [\[CrossRef\]](#)
47. Powell, M.D.; Dodge, P.P.; Black, M.L. The landfall of Hurricane Hugo in the Carolinas: Surface wind distribution. *Weather Forecast.* **1991**, *6*, 379–399. [\[CrossRef\]](#)
48. Senkbeil, J.C.; Myers, L.; Jasko, S.; Reed, J.R.; Mueller, R. Communication and hazard perception lessons from category five hurricane michael. *Atmosphere* **2020**, *11*, 804. [\[CrossRef\]](#)

49. Kaplan, J.; DeMaria, M. A simple empirical model for predicting the decay of tropical cyclone winds after landfall. *J. Appl. Meteorol.* **1995**, *34*, 2499–2512. [CrossRef]
50. Moore, T.W.; Dixon, R.W. Climatology of tornadoes associated with Gulf Coast-landfalling hurricanes. *Geogr. Rev.* **2011**, *101*, 371–395. [CrossRef]
51. Rhodes, C.L.; Senkbeil, J.C. Factors contributing to tornadogenesis in landfalling Gulf of Mexico tropical cyclones. *Meteorol. Appl.* **2014**, *21*, 940–947. [CrossRef]
52. Deo, A.A.; Ganer, D.W. Tropical cyclone activity over the Indian Ocean in the warmer climate. In *Monitoring and Prediction of Tropical Cyclones in the Indian Ocean and Climate Change*; Springer: Dordrecht, The Netherlands, 2014; pp. 72–80.
53. Krishnamohan, K.S.; Mohanakumar, K.; Joseph, P. V Climate change in tropical cyclones and monsoon depressions of North Indian Ocean. In *Monitoring and Prediction of Tropical Cyclones in the Indian Ocean and Climate Change*; Springer: Dordrecht, The Netherlands, 2014; pp. 33–39.
54. Yin, J.; Yin, Z.; Xu, S. Composite risk assessment of typhoon-induced disaster for China's coastal area. *Nat. Hazards* **2013**, *69*, 1423–1434. [CrossRef]
55. Cao, C.; Xu, P.; Wang, Y.; Chen, J.; Zheng, L.; Niu, C. Flash flood hazard susceptibility mapping using frequency ratio and statistical index methods in coalmine subsidence areas. *Sustainability* **2016**, *8*, 948. [CrossRef]
56. Hossain, M.K.; Meng, Q. A fine-scale spatial analytics of the assessment and mapping of buildings and population at different risk levels of urban flood. *Land Use Policy* **2020**, *99*, 104829. [CrossRef]
57. Rappaport, E.N.; Fernandez-Partagas, J. *The Deadliest Atlantic Tropical Cyclones*; National Hurricane Center: Washington, DC, USA, 1995; pp. 1492–1994.
58. Blake, E.S.; Rappaport, E.N.; Landsea, C.W. *The Deadliest, Costliest, and most Intense United States Tropical Cyclones from 1851 to 2006 (and Other Frequently Requested Hurricane Facts)*; NOAA/National Weather Service, National Centers for Environmental Prediction: Washington, DC, USA, 2007.
59. Burroughs, W.J. *Climate Change: A Multidisciplinary Approach*; Cambridge University Press: Cambridge, UK, 2007; ISBN 1107049253.
60. Camp, J.; Scaife, A.A.; Heming, J. Predictability of the 2017 North Atlantic hurricane season. *Atmos. Sci. Lett.* **2018**, *19*, 1–7. [CrossRef]
61. Lavender, S.L.; Walsh, K.J.E.; Caron, L.P.; King, M.; Monkiewicz, S.; Guishard, M.; Zhang, Q.; Hunt, B. Estimation of the maximum annual number of North Atlantic tropical cyclones using climate models. *Sci. Adv.* **2018**, *4*, 1–8. [CrossRef]
62. Doss, D.A.; Mcelreath, D.; Goza, R.; Tesiero, R.; Gokaraju, B.; Henley, R. Assessing the Recovery Aftermaths of Selected Disasters in the Gulf of Mexico. *Logist. Sustain. Transp.* **2018**, *9*, 1–10. [CrossRef]
63. Czajkowski, J.; Villarini, G.; Michel-Kerjan, E.; Smith, J.A. Determining tropical cyclone inland flooding loss on a large scale through a new flood peak ratio-based methodology. *Environ. Res. Lett.* **2013**, *8*. [CrossRef]
64. Wang, H.; Xu, M.; Onyejuruwa, A.; Wang, Y.; Wen, S.; Gao, A.E.; Li, Y. Tropical cyclone damages in Mainland China over 2005–2016: Losses analysis and implications. *Environ. Dev. Sustain.* **2019**, *21*, 3077–3092. [CrossRef]
65. Gemmer, M.; Yin, Y.; Luo, Y.; Fischer, T. Tropical cyclones in China: County-based analysis of landfalls and economic losses in Fujian Province. *Quat. Int.* **2011**, *244*, 169–177. [CrossRef]
66. Rifat, S.A.A.; Liu, W. Measuring Community Disaster Resilience in the Conterminous Coastal United States. *ISPRS Int. J. Geo Inf.* **2020**, *9*, 469. [CrossRef]
67. García-Ayllón, S.; Tomás, A.; Ródenas, J.L. The spatial perspective in post-earthquake evaluation to improve mitigation strategies: Geostatistical analysis of the seismic damage applied to a real case study. *Appl. Sci.* **2019**, *9*, 3182. [CrossRef]
68. Sung, C.H.; Liaw, S.C. A GIS-based approach for assessing social vulnerability to flood and debris flow hazards. *Int. J. Disaster Risk Reduct.* **2020**, *46*, 101531. [CrossRef]
69. Yoon, D.K.; Kang, J.E.; Brody, S.D. A measurement of community disaster resilience in Korea. *J. Environ. Plan. Manag.* **2016**, *59*, 436–460. [CrossRef]
70. Cutter, S.L.; Ash, K.D.; Emrich, C.T. The geographies of community disaster resilience. *Glob. Environ. Chang.* **2014**, *29*, 65–77. [CrossRef]
71. Roth, D. Tropical Cyclone Rainfall Duration and Maxima. Available online: <https://www.wpc.ncep.noaa.gov/tropical/rain/tcduration.html> (accessed on 9 May 2017).
72. Cai, H.; Lam, N.S.N.; Zou, L.; Qiang, Y.; Li, K. Assessing community resilience to coastal hazards in the Lower Mississippi River Basin. *Water* **2016**, *8*, 46. [CrossRef]
73. Hair, J.F.; Black, W.C.; Babin, B.J.; Anderson, R.E.; Tatham, R.L. *Multivariate Data Analysis*; DigitalCommons: Prentice Hall, NJ, USA, 1998; Volume 5.
74. Zhao, C.; Jensen, J.; Weng, Q.; Weaver, R. A geographically weighted regression analysis of the underlying factors related to the surface Urban Heat Island Phenomenon. *Remote Sens.* **2018**, *10*, 1428. [CrossRef]
75. Matyas, C.J. Processes influencing rain-field growth and decay after tropical cyclone landfall in the United States. *J. Appl. Meteorol. Climatol.* **2013**, *52*, 1085–1096. [CrossRef]
76. Andersen, T.K.; Shepherd, J.M. A global spatiotemporal analysis of inland tropical cyclone maintenance or intensification. *Int. J. Climatol.* **2014**, *34*, 391–402. [CrossRef]

-
77. Evans, C.; Schumacher, R.S.; Galarneau, T.J., Jr. Sensitivity in the overland reintensification of Tropical Cyclone Erin (2007) to near-surface soil moisture characteristics. *Mon. Weather Rev.* **2011**, *139*, 3848–3870. [[CrossRef](#)]
 78. Kellner, O.; Niyogi, D.; Lei, M.; Kumar, A. The role of anomalous soil moisture on the inland reintensification of Tropical Storm Erin (2007). *Nat. Hazards* **2012**, *63*, 1573–1600. [[CrossRef](#)]
 79. Baker, A. *Creating an Empirically Derived Community Resilience Index of the Gulf of Mexico Region*; Louisiana State University: Baton Rouge, LA, USA, 2009.
 80. Kossin, P.A. Global Slowdown of Tropical Cyclone Translational-Speed. *Nature* **2018**, *558*, 104–107. [[CrossRef](#)] [[PubMed](#)]
 81. Wang, S.Y.S.; Yoon, J.H.; Klotzbach, P.; Gillies, R.R. Quantitative attribution of climate effects on Hurricane Harvey's extreme rainfall in Texas. *Environ. Res. Lett.* **2018**, *5*, 13. [[CrossRef](#)]
 82. Chan, K.T.F. Are global tropical cyclones moving slower in a warming climate? *Environ. Res. Lett.* **2019**, *10*, 14. [[CrossRef](#)]
 83. Hassanzadeh, P.; Lee, C.Y.; Nabizadeh, E.; Camargo, S.J.; Ma, D.; Yeung, L.Y. Effects of climate change on the movement of future landfalling Texas tropical cyclones. *Nat. Commun.* **2020**, *11*, 1. [[CrossRef](#)] [[PubMed](#)]